NANO LETTERS

2004
Vol. 4, No. 8
1401−1406

Polarized Absorption and Emission of Ordered Self-Assembled Porphyrin Rings

Cécile R. L. P. N. Jeukens,[†] Marga C. Lensen,[‡] Frans J. P. Wijnen,[†] Johannes A. A. W. Elemans,[‡,§] Peter C. M. Christianen,*[,†] Alan E. Rowan,[‡] Jan W. Gerritsen,[§] Roeland J. M. Nolte,[‡] and Jan C. Maan[†]

NSRIM, High Field Magnet Laboratory HFML, University of Nijmegen, Toernooiveld 7, 6525 ED NIJMEGEN, The Netherlands, NSRIM, Department of Organic Chemistry, University of Nijmegen, Toernooiveld 1, 6525 ED NIJMEGEN, The Netherlands, and NSRIM, Department of Solid State Physics, University of Nijmegen, Toernooiveld 1, 6525 ED NIJMEGEN, The Netherlands

Received April 30, 2004; Revised Manuscript Received June 2, 2004

ABSTRACT

Self-assembled rings (with diameters of 0.1−2.0 μm) consisting of porphyrin dodecamer molecules are formed by evaporating chloroform solutions on glass substrates. Fluorescence microscopy experiments on individual rings reveal a strongly polarized optical absorption and emission. Quantitative analysis of the fluorescence images evidences the high degree of order within the rings, consisting of radially oriented columnar stacks of porphyrin dodecamers, and the absence of energy transport along the rings on length scales resolved by fluorescence microscopy.

The fabrication of well-defined nanoscale objects is essential for the understanding and development of novel potentially useful materials. These systems differ substantially from the corresponding bulk material, because their properties are closely related to the actual dimensions, shape, and composition. In recent years several nanostructures have been produced, varying from rods,[1] wires,[2−4] and tubes[5,6] to dots,[7,8] rings,[9−13] and vesicles,[14] composed of both inorganic and organic materials. The use of organic molecules as building blocks is very promising because they provide a relatively easy, low-cost, and versatile means to construct nanostructures with a desired shape and functionality, taking advantage of molecular self-assembly processes. In this letter, we report the fabrication of porphyrin-based, ring-shaped supramolecular architectures with a pronounced polarized optical response that results from the highly ordered arrangement of molecular nanoaggregates within the rings.

Symmetric ring-shaped structures are relevant to test fundamental concepts such as trapping of magnetic flux and (coherent) transport of charge or energy. Therefore, many researchers have constructed and studied nanosized rings of metals,[15,16] semiconductors,[9] carbon nanotubes,[12,13] magnetic nanoparticles,[17] and organic molecules,[10,11,18,19] or isolated and investigated circular arrays occurring in nature, such as the light harvesting complexes LH1 and LH2.[20] In these latter complexes porphyrin molecules are organized in a precise circular arrangement beneficial for an efficient absorption of photons and the subsequent transfer of energy. The formation of well-defined multiporphyrin ring-shaped arrays provides, therefore, an essential first step toward the realization of artificial light-harvesting systems. Furthermore, porphyrins in general possess (photo-)catalytic, electronic, optical, and magnetic properties that are suitable for a wide range of applications.

Porphyrin-based molecules can be equipped with handles for molecular recognition and programmed to self-assemble into larger supramolecular architectures of predefined morphology, driven by noncovalent interactions such as hydrogen bonding, $\pi-\pi$ interactions, and van der Waals interactions.[21] In practice, ring-shaped architectures can be made on a surface out of an evaporating solution. The final result is determined by a complex interplay between the design of the molecules used as building blocks, the (de)wetting properties of the substrate and the solvent, and other local conditions.[10,11,18,19,22−24] The ring formation process can be improved by increasing the π-surface of the constituting molecules, which is evidenced by better ring formation of

* Corresponding author. E-mail: peterc@sci.kun.nl.
† High Field Magnet Laboratory.
‡ Department of Organic Chemistry.
§ Department of Solid State Physics.

10.1021/nl049363d CCC: $27.50
Published on Web 07/01/2004

porphyrin hexamers (six porphyrin moieties coupled to a central benzene ring) as compared to porphyrin dimers.[10,11,18,19] Recently, we have achieved a considerable enhancement of the degree of molecular order within the rings by optimizing the (de)wetting properties of the supporting surface.[24] The internal order of rings consisting of porphyrin hexamer molecules prepared on a hydrophilic glass substrate was observed by the polarization of the fluorescence emission. In this letter, we further increase the π-surface of the constituting molecules by using porphyrin dodecamer molecules (containing twelve porphyrin moieties) and find that this step leads to the formation of highly ordered rings, exhibiting a very high degree of optical polarization, as well as a very narrow size distribution. The ring formation is rather independent of the wettability of the surface, since ordered rings are formed on both hydrophilic and hydrophobic glass plates. The observed optical polarization is due to radially directed columnar stacks of porphyrin dodecamers. We can determine the ordering of these stacks by comparing the experimental polarization degree with a theoretical model taking into account the absorption and emission of the dipole transition moments and including a certain degree of orientational disorder.

The porphyrin dodecamer molecules used as molecular building blocks consist of twelve porphyrin moieties attached to a rigid core (see Figure 1a for the three-dimensional structure and the dimensions) and have a strong tendency to form columnar stacks due to strong intermolecular $\pi-\pi$ interactions.[25] Ring-shaped supramolecular arrays were prepared following a procedure that was extensively discussed before[10,11,18,19,24] and which is only briefly outlined here: drop-casting 3 μL of a ~5 μM porphyrin dodecamer solution in chloroform on a substrate results in a film that thins due to evaporation of the solvent. Under a critical thickness the film becomes unstable and ruptures, leading to the development of pinholes that slowly grow in size. This process is accompanied by a net flow of solute toward the pinhole because the evaporation rate at the rim of the hole is higher than in the film. As the concentration of molecules increases, aggregation of the molecules occurs, leading to the deposition of ring-shaped structures around the pinhole when the solvent is completely evaporated. We find that well-defined rings form on both hydrophilic and hydrophobic glass substrates (see ref 24 for details on the surface preparation), at a relative humidity of 65% or higher, at ambient temperatures and for a concentration range of 0.1 to 170 μM. Using substrates such as highly oriented pyrolytic graphite, untreated glass or mica leads to a network of merged rings or no rings at all, whereas a low relative humidity also prohibits ring formation. The samples are stable over a period of at least 10 weeks.

The dimensions of the ring-shaped architectures were characterized using atomic force microscopy[26] (AFM). A typical AFM image of the rings on a hydrophilic glass substrate (Figure 1b) shows many regular rings of roughly the same size. A histogram of ring-diameters (Figure 1c), taken from 193 rings within an area of ~2000 μm^2, is a narrow Gaussian distribution centered around 1.4 μm with

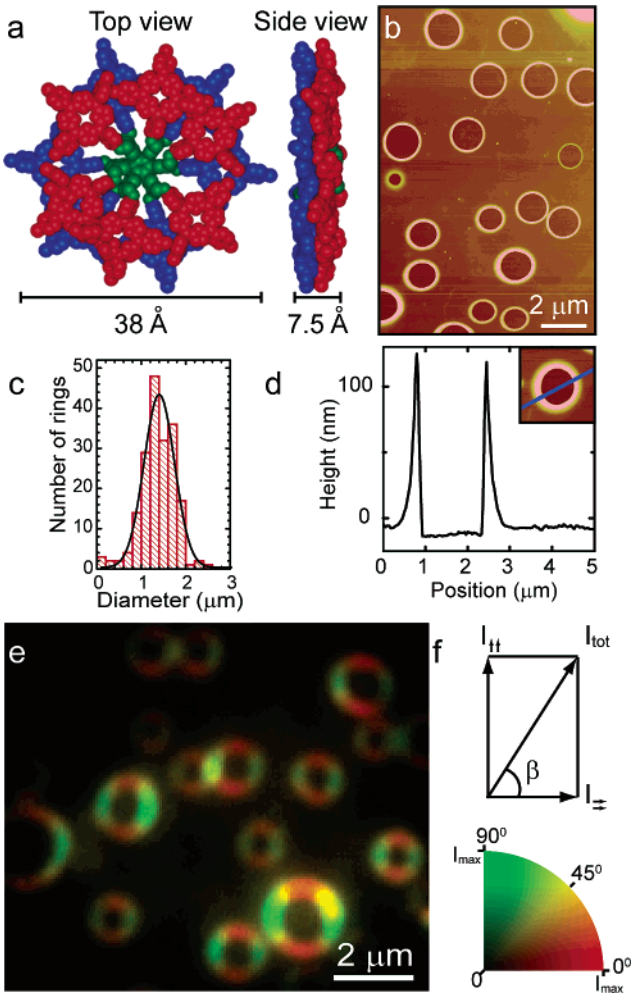

Figure 1. (a) Three-dimensional representation of the porphyrin dodecamer molecule with its dimensions; (b) AFM image of dodecamer rings on a hydrophilic substrate, the scale bar represents 2 μm; (c) histogram showing the size distribution of 193 rings within an area of ~2000 μm^2, partly shown in the AFM image of (b). The average size is 1.4 μm, the fwhm of the Gaussian fit (solid line) is 0.7 μm. (d) Cross section through a typical ring in the same area as (b) and (c) (along the line, see inset) showing a steep inner rim in contrast to the shallow outer rim; (e) polarized FM image using a color coding (f) via a calculation of the polarization angle β out of two successive measurements with polarization horizontal ($I_{\rightarrow\rightarrow}$) and vertical ($I_{\uparrow\uparrow}$). All rings show a strongly polarized optical response.

a width of 0.7 μm. In this area the average wall thickness is 300 nm and the average height 85 nm. We have observed many regions with well-defined, uniformly sized rings on all samples on both hydrophilic and hydrophobic glass, although the average diameter was found to vary from area to area, ranging from 100 nm to 1.8 μm. The cross-section of a typical ring located in the area of Figure 1b reveals a steep interior rim and a shallow outside rim (Figure 1d), which confirms the pinhole formation mechanism. According to this mechanism the molecules are delivered from outside the pinhole toward its rim, implying that no molecules are deposited within the pinhole (ring). This finding was further confirmed by near-field scanning optical microscopy experiments in illumination mode[27] where no emission from the inside of the rings was observed (image not shown). By far,

most of the cyclic arrays are well-defined and are situated in an area with a sharp size distribution, suggesting a highly controlled formation mechanism triggered by spinodal dewetting,[24,28,29] in contrast to dewetting by heterogeneous nucleation sites that leads to randomly sized rings, exhibiting defects or irregularities.

The high degree of internal molecular ordering within the rings is demonstrated by the polarized fluorescence microscopy[30] (FM) image in Figure 1e. This image is constructed from two consecutive measurements, with both excitation and detection polarizations either vertical or horizontal. To denote the orientation of the polarizers, we use ↑ or → for vertical or horizontal polarization, respectively. These symbols are put between brackets to define the excitation and detection polarization, i.e., (↑↑) means parallel vertical excitation and detection, etc. Using simple vector algebra, the polarization angle of the light can be determined and is plotted using the two extremal colors red (0°) and green (90°) and the intermediate color yellow (45°) (Figure 1f). All rings within the excitation area emit horizontally polarized light at the upper and bottom parts (red), whereas the light is vertically polarized (green) at the left and right parts. This indicates that the optical dipole moments of the porphyrin molecules are arranged in a well-ordered fashion, namely tangentially to the ring. The molecules are excited using a laser with a wavelength of 457.9 nm, which is within the so-called Soret band. Irrespective of the position on the ring, the fluorescence spectrum always shows two peaks at 662 and 723 nm, originating from the Q-bands.[31] It is well-known that both the Soret band and the Q-band transition moments of single porphyrin molecules are directed in the plane of the molecule.[32] Since the dodecamer molecules contain twelve porphyrins that are proposed to be oriented within one plane (Figure 1a),[25] also the absorption and emission dipole moments of the dodecamer molecule are in the plane, which implies that the FM polarization data is consistent only with molecules that are tangentially aligned along the ring.

To determine the degree of order within the rings we performed a quantitative analysis of the FM results (Figure 2). Figure 2a and b shows false color FM images of the original measurements (↑↑) and (→ →), respectively, of a typical ring of 1.25 μm diameter, as well as the image recorded with crossed polarizers (↑→) (Figure 2c). The data are quantified in Figure 2g by plotting the fluorescence intensity along the ring as a function of angle φ (Figure 2f) for the three depicted polarization images: black (↑↑), red (→ →) and blue (↑→) symbols. These traces are all normalized to the total fluorescence intensity (↑↑ + → →), yielding values between 0 and 1. The high degree of polarization is evident from the results in Figure 2g, displaying sinusoidal curves oscillating between 0.13 and 0.87, symmetric around half the intensity (0.5). Furthermore, the (↑↑) and (→ →) curves are perfectly in anti-phase, evidencing the circular symmetry of the optical response, and they have their maxima and minima at 0°, 90°, 180°, and 270°, confirming the tangential alignment of the molecules. The maximum intensity of the cross-polarized curve (↑→) is reduced by a factor of 2 as compared to the maximum intensity of the

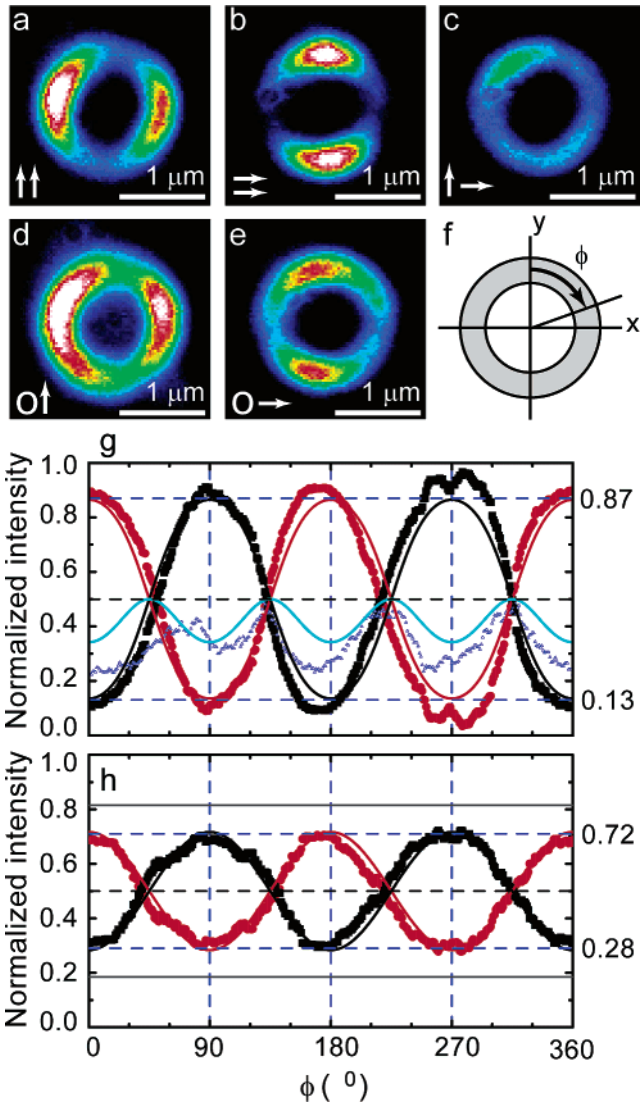

Figure 2. False color FM image of a single 1.25 μm-diameter ring for excitation and detection polarization oriented (a) both vertical (↑↑), (b) both horizontal (→ →), (c) vertical excitation and horizontal detection (↑→), (d) unpolarized excitation and vertical detection (O↑), (e) unpolarized excitation and horizontal detection (O→). Images a, b, and c are plotted on the same color scale, different from that of d and e. (f) Definition of the angle φ; (g, h) fluorescence intensity along the ring. The symbols are the data: (g) black (↑↑), red (→ →), and blue (↑→) and (h) black (O↑), and red (O→). The solid lines are model calculations, which are described in more detail in the text. The gray lines in (h) are the maximum and minimum polarization intensities achievable using a N.A. = 0.9 microscope objective.

(↑↑) and (→ →) curves, while its minimum intensity is higher. In fact, the (↑→) trace exhibits four maxima that coincide with the crossing points of the (↑↑) and (→ →) curves. Finally, the solid lines in Figure 2g are the results of model calculations that will be discussed below.

The optical response in Figures 1e and 2a, b, and c is determined by both the excitation and detection polarization and possibly energy transfer. If energy transfer occurs, optical absorption at one point in the rings leads to emission from a larger area due to exciton migration. Our polarization data implicitly contain this information since the excitation

Table 1. Minimum and Maximum Values of the Intensity of the (↑↑) and (→→) Polarization Curves as Well as the (O↑) and (O→) Curves for Six Different Rings Having a Diameter Stated in the First Column

	(↑↑) & (→→)		(O↑) & (O→)		
size (μm)	min	max	min	max	Δ^a
1.25	0.13	0.87	0.28	0.72	19°
2.13	0.15	0.85	0.32	0.68	23°
1.31	0.19	0.81	0.33	0.67	25°
0.78	0.37	0.63	0.34	0.66	26°
1.69	0.27	0.73	0.38	0.62	32°
0.94	0.34	0.66	0.39	0.61	33°
perfect ring[b]	0.05	0.95	0.18	0.82	0°

[a] Value of the parameter Δ used in the calculations for describing the data, including the depolarizing effect of using a N.A. = 0.9 microscope objective. [b] Values calculated for a perfectly ordered ring.

polarization defines limited areas of absorption in the rings. To disentangle these effects, we have also measured rings using either unpolarized (denoted by 'O') excitation or detection polarization (see Figures 2d and e for the false color (O↑) and (O→) FM images). The (O↑) and (O→) curves (Figure 2h, normalized to (O↑) + (O→)), and the normalized (↑O) and (→O) curves (not shown) all show an equal phase and an amplitude defined by $I_{min} = 0.28$ and $I_{max} = 0.72$, which is smaller as compared to the (↑↑) and (→→) curves. The fact that (↑O) and (→O) curves are equal to, respectively, the (O↑) and (O→) traces confirms that indeed the absorption (Soret band) and emission (Q-band) dipole moments are parallel, and moreover, that on the scale resolved by our experiment no energy transfer occurs. Finally, we have verified that this complete dataset is consistent by checking that the experimental (↑↑) and (→→) curves coincide with the curves calculated according to (↑O) × (O↑) = (↑↑) and (→O) × (O→) = (→→). We have performed this extensive optical analysis on six rings of different sizes, yielding values for the minimum and maximum fluorescence intensities summarized in Table 1. The measured intensity values for (↑↑) and (→→) polarization and (O↑) and (O→) polarization are all consistent with each other, except for the 0.78 μm sized ring. Indeed, all rings show a pronounced optical polarization, although the polarization degree varies from ring to ring. In the following we consider the polarized emission of the rings to determine the internal ordering, i.e., we use I_{min} and I_{max} of the (O↑) and (O→) curves.

For a perfectly ordered ring, the polarization is expected to be complete, i.e., $I_{max} = 1.0$ and $I_{min} = 0.0$, which is significantly higher than the experimental values of $I_{max} = 0.72$ and $I_{min} = 0.28$. In the following, we will show that this deviation can be explained partially by the experimental configuration of the optical microscopy setup and partially by ring imperfections. We therefore simulate our FM results by a relatively simple model calculation, which accounts for these effects. The optical response of rings is modeled by summing up optical dipoles at the molecular level, where each dodecamer molecule is represented by the sum of two perpendicular dipoles (Figures 3a and b), which is reasonable since the constituting dipole moments of the twelve porphyrins are evenly distributed in the plane of the molecule. Each

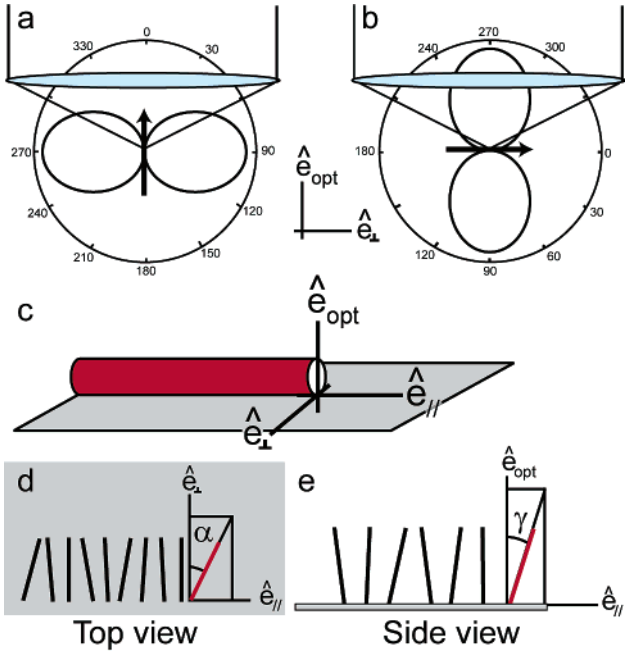

Figure 3. Orientation of the dipoles and dipole fields within one molecule (a) dipole parallel to the optical axis, and (b) dipole in plane of the surface. Also drawn is the collection cone of a N.A. = 0.9 microscope objective. (c) Schematic representation of a stack of molecules and the used coordinate axes. Definition of the rotation angles (d) α and (e) γ. See text for more details.

dipole has a donut-shaped radiation field with an electric field $\vec{E}(\theta) = E_0 \cdot \sin(\theta) \cdot \hat{e}_\theta$, where θ is the angle with the dipole axis, defined in spherical coordinates[33] and E_0 is a constant. The direction of the light ray with an electric field $\vec{E}(\theta)$ is given by the spherical unit vector $\hat{e}_r$.

Using a high numerical aperture (N.A.) microscope objective for collecting the light has a considerable effect on the measured polarization. The N.A. is a measure of the solid angle covered by the objective. The fluorescence is detected in reflection geometry, through air, i.e., without a cover glass, using a 100× air objective with N.A. = 0.9, which corresponds to a half-top cone angle of 64°. Such a large cone angle allows the collection of a considerable amount of light emanating from dipoles oriented parallel to the optical axis, perpendicular to the glass substrate (Figure 3a, where the collection cone of the objective is schematically drawn).[34,35] Since the field ($\vec{E}_{opt}$) of these dipoles is symmetric around the optical axis, their contribution to the fluorescence is unpolarized, in contrast to the emission ($\vec{E}_\perp$) of dipoles directed in the plane of the substrate (Figure 3b) which is almost completely linearly polarized. A high N.A. objective therefore limits the maximum polarization that can be observed. In the case of a N.A. = 0.9 objective, we calculated that a perfectly ordered ring displays a maximum polarization of $I_{max} = 0.82$ and $I_{min} = 0.18$ (indicated by the gray lines in Figure 2h), which accounts for part of the lack of complete polarization in the FM polarization data.

To have a full description of the observed FM polarization, we consider a realistic model of columnar stacks of porphyrin dodecamer molecules[25] forming the ring, schematically

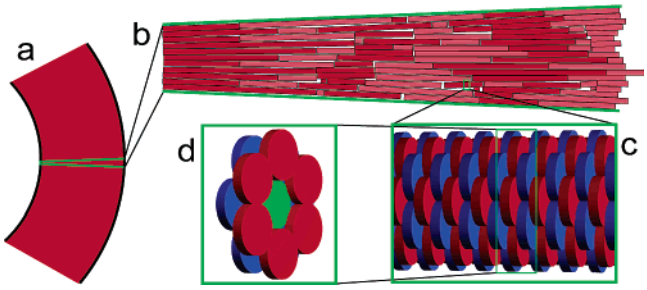

Figure 4. Proposed internal structure of the rings, all pictures are to scale. (a) Segment of the ring; (b) a close-up of the orientation of the stacks in the ring. Two colors are used to facilitate the distinction between the stacks. (c) Orientation of the molecules in a stack; d) schematic representation of a single porphyrin dodecamer.

depicted in Figure 4. Given the measured wall thickness of a typical ring (300 nm), we propose that the ring is likely to consist of several stacks with a certain distribution in lengths that are all aligned radially (see Figure 4b, which is an image to scale). The height of a typical ring (85 nm) implies that there are about 20−30 stacks on top of each other. Small deviations of stacks from the perfectly radial direction and of individual molecules with respect to the stack direction lead to a depolarization of the fluorescence. In our model we include this type of disorder by allowing molecules to rotate over two angles α and γ with respect to the stack direction (Figure 3c shows a schematic representation of a stack and the definition of the axes). The angle α (Figure 3d) corresponds to a rotation about the optical axis ($\hat{e}_{opt}$), i.e., in the $\hat{e}_{\perp},\hat{e}_{||}$-plane, and the angle γ (Figure 3e) is a rotation about the $\hat{e}_{\perp}$-axis, i.e., in the $\hat{e}_{||},\hat{e}_{opt}$ plane. In our model the molecules are allowed to rotate with angles α and γ according to Gaussian distributions $D(\alpha)$ and $D(\gamma)$ with widths $\Delta\alpha$ and $\Delta\gamma$, i.e., for α: $D(\alpha) = C\cdot\exp(-\alpha^2/2\Delta\alpha^2)$, where C is a normalization constant. These distributions can represent either static spatial distributions of molecules within stacks, misorientation of stacks as a whole, or dynamic, time-averaged distributions of molecules fluctuating around the (perfectly ordered) equilibrium positions. In principle, this model can be used to determine the degree of internal order of any solid-state architecture built up by chromophores on a surface.

The intensity of the collected light with horizontal ($= \hat{e}_x$-direction) or vertical polarization ($= \hat{e}_y$-direction) is calculated by integrating the expressions $|(\vec{E}_{opt} + \vec{E}_{\perp})\cdot\hat{e}_x|^2$ and $|(\vec{E}_{opt} + \vec{E}_{\perp})\cdot\hat{e}_y|^2$ over the space covered by the collection cone of the objective. These two expressions are multiplied by $D(\alpha)$ and $D(\gamma)$ and integrated over α and γ, thereby assuming that $\Delta\alpha = \Delta\gamma = \Delta$, which leaves Δ as the only fitting parameter. The calculation is done for an angle φ ranging from 0° to 360°. This procedure is used to calculate the (O↑) and (O→) curves, the (↑↑) and (→ →) curves (by taking the square of each expression), and the (↑→) curve (by multiplying both expressions). We find that a value of $\Delta = 19°$ can perfectly describe the precise shape and amplitude of all the FM polarization traces (solid lines in Figures 2g and h) of the ring in Figure 2. Similar results are obtained for the other rings (see Table 1) using slightly higher values for Δ.

The low values found for Δ reflect the high internal molecular order of the rings, which is a striking conclusion considering the rather crude method of preparation. Apparently the combined action of the pinhole formation mechanism, triggered by spinodal dewetting, accompanied by molecular self-assembly, provides a high level of control. In general the values found for Δ in the case of porphyrin dodecamer are much lower than those for the hexamers (minimal $\Delta = 35°$) used in previous studies,[24] clearly showing that the increased π-surface of the dodecamer molecules increases the stacking interactions. In fact, we anticipate that the polarization of the fluorescence might improve even more at lower temperatures, when thermal fluctuations are suppressed, which may also cause apparent depolarization.

In conclusion, we have demonstrated that we have achieved control over the self-assembly process of porphyrin molecules into ring-shaped architectures. Rings formed on both hydrophilic and hydrophobic glass substrates have a very uniform size distribution, and FM measurements reveal their highly polarized absorption and emission. Quantitative analysis evidences that the degree of order of the molecules in the radially oriented stacks is high. These rings provide model systems for the investigation of energy transfer, optical waveguiding, and might find an application in catalysis. In this regard, experiments performed at lower (helium) temperatures, or with higher optical resolution (NSOM) are feasible to detect energy transfer and optical waveguiding. Alternatively, the introduction of compatible porphyrin derivatives or other molecules, with slightly shifted emission lines, in a ring or its interior, provides exciton traps that can be isolated spectrally and therefore can be used to monitor energy transfer in either radial or tangential directions. Finally, well-ordered ring-shaped structures composed of porphyrins containing transition metals can serve as special types of heterogeneous catalysts.

Acknowledgment. The Stichting voor Fundamenteel Onderzoek der Materie (FOM), financially supported by the Nederlandse Organisatie voor Wetenschappelijk Onderzoek (NWO), and the National Research School Combination: Catalysis are acknowledged for financing.

References

(1) Nicewarner-Peña, S. R.; Freeman, R. G.; Reiss, B. D.; He, L.; Peña, D. J.; Walton, I. D.; Cromer, R.; Keating, C. D.; Natan, M. J. *Science* **2001**, *294*, 137.
(2) Gudiksen, M. S.; Lauhon, L. J.; Wang, J.; Smith, D. C.; Lieber, C. M. *Nature* **2002**, *415*, 617.
(3) Higgins, D. A.; Kerimo, J.; Vanden Bout, D. A.; Barbara, P. F. *J. Am. Chem. Soc.* **1996**, *118*, 4049.
(4) Jonkheijm, P.; Hoeben, F. J. M.; Kleppinger, R.; van Herrikhuyzen, J.; Schenning, A. P. H. J.; Meijer, E. W. *J. Am. Chem. Soc.* **2003**, *125*, 15941.
(5) Kong, J.; Soh, H. T.; Cassell, A. M.; Quata, C. F.; Dai, H. *Nature* **1998**, *395*, 878.
(6) Rueckes, T.; Kim, K.; Joselevich, E.; Tseng, G. Y.; Cheung, C.-L.; Lieber, C. M. *Science* **2000**, *289*, 94.
(7) Kouwenhoven, L.; Marcus, C. *Phys. World* **1998**, *June*, 35.
(8) Bayer, M.; Stern, O.; Hawrylak, P.; Fafard, S.; Forchel, A. *Nature* **2000**, *405*, 923.

(9) Warburton, R. J.; Schäflein, C.; Haft, D.; Bickel, F.; Lorke, A.; Karrai, K.; Garcia, J. M.; Schoenfeld, W.; Petroff, P. M. *Nature* **2000**, *405*, 926.
(10) Schenning, A. P. H. J.; Benneker, F. B. G.; Geurts, H. P. M.; Liu, X. Y.; Nolte, R. J. M. *J. Am. Chem. Soc.* **1996**, *118*, 8549.
(11) Latterini, L.; Blossey, R.; Hofkens, J.; Vanoppen, P.; de Schryver, F. C.; Rowan, A. E.; Nolte, R. J. M. *Langmuir* **1999**, *15*, 3582.
(12) Tans, S. J.; Dekker, C. *Nature* **1997**, *385*, 780.
(13) Sano, M.; Kamino, A.; Okamura, J.; Shinkai, S. *Science* **2001**, *293*, 1299.
(14) Vriezema, D. M.; Hoogboom, J.; Velonia, K.; Takazawa, K.; Christianen, P. C. M.; Maan, J. C.; Rowan, A. E.; Nolte, R. J. M. *Angew. Chem., Int. Ed.* **2003**, *42*, 772.
(15) Aizpurua, J.; Hanarp, P.; Sutherland, D. S.; Käll, M.; Bryant, G. W.; García de Abajo, F. J. *Phys. Rev. Lett.* **2003**, *90*, 057401.
(16) Lévy, L. P.; Dolan, G.; Dunsmuir, J.; Bouchiat, H. *Phys. Rev. Lett.* **1990**, *64*, 2074.
(17) Tripp, S. L.; Pusztay, S. V.; Ribbe, A. E.; Wei, A. *J. Am. Chem. Soc.* **2002**, *124*, 7914.
(18) Biemans, H. A. M.; Rowan, A. E.; Verhoeven, A.; Vanoppen, P.; Latterini, L.; Foekema, J.; Schenning, A. P. H. J.; Meijer, E. W.; de Schryver, F. C.; Nolte, R. J. M. *J. Am. Chem. Soc.* **1998**, *120*, 11054.
(19) Foubert, P.; Vanoppen, P.; Martin, M.; Gensch, T.; Hofkens, J.; Helser, A.; Seeger, A.; Taylor, R. M.; Rowan, A. E.; Nolte, R. J. M.; de Schryver, F. C. *Nanotechnology* **2000**, *11*, 16.
(20) van Oijen, A. M.; Ketelaars, M.; Köhler, J.; Aartsma, T. J.; Schmidt, J. *Science* **1999**, *285*, 400.
(21) Lehn, J.-M. *Supramolecular Chemistry*, VCH: Weinheim, 1995.
(22) Ohara, P. C.; Gelbart, W. M. *Langmuir* **1998**, *14*, 3418.
(23) Balzer, F.; Beermann, J.; Bozhevolnyi, S. I.; Simonsen, A. C.; Rubahn, H.-G. *Nano Lett.* **2003**, *3*, 1311.
(24) Lensen, M. C.; Takazawa, K.; Elemans, J. A. A. W.; Jeukens, C. R. L. P. N.; Christianen, P. C. M.; Maan, J. C.; Rowan, A. E.; Nolte, R. J. M. *Chem. Eur. J.* **2004**, *10*, 831.
(25) Lensen, M. C.; van Dingenen, S. J. T.; Elemans, J. A. A. W.; Dijkstra, H. P.; van Klink, G. P. M.; van Koten, G.; Gerritsen, J. W.; Speller, S.; Nolte, R. J. M.; Rowan, A. E. *Chem. Commun.* **2004**, *7*, 762.
(26) We use an atomic force microscope (Digital Instruments, Nanoscope IIIa) in tapping mode at room temperature, in air, using NSG-10 (NT-MDT) silicon cantilevers.
(27) Details on the principles of the NSOM technique, which is an optical scanning probe technique that achieves an optical resolution of ~100 nm, can be found in the following review papers: Dunn, R. C. *Chem. Rev.* **1999**, *99*, 2891; Hecht, B.; Sick, B.; Wild, U. P.; Deckert, V.; Zenobi, R.; Martin, O. J. F.; Pohl, D. W. *J. Chem. Phys.* **2000**, *112*, 7761; De Serio, M.; Zenobi, R.; Deckert, V. *Trac.-Trend Anal. Chem.* **2003**, *22*, 70.
(28) Mertig, M.; Thiele, U.; Bradt, J.; Klemm, D.; Pompe, W. *Appl. Phys. A* **1998**, *66*, S565.
(29) Thiele, U.; Velarde, M. G.; Neuffer, K. *Phys. Rev. Lett.* **2001**, *87*, 016104.
(30) Fluorescence microscopy images were made by focusing the output of an argon ion laser (λ = 457.9 nm) by a 100× or 50× Zeiss objective to a ~15 μm spot. The polarization of the excitation laser beam could be changed without affecting the excitation volume by using a combination of a Glan-Taylor polarizer and a Babinet-Soleil compensator. The fluorescence emitted by the sample was collected by the same objective and guided through a dichroic mirror and long-pass filter to eliminate the direct reflection of the laser light. The fluorescence was imaged on an air-cooled intensified CCD-camera (Pimax, 512 × 512 pixels) through a Glan-Taylor polarizer, resulting in a diffraction-limited image (resolution $\sim\lambda/2 \approx$ 300 nm for the 100× objective). The excitation power was $p \approx 800$ mWcm^{-2}, which is sufficiently low to avoid bleaching. The capture time was 20−30 s, using an intensifier gain of 150.
(31) White, W. I. *The Porphyrins*; Academic Press: New York, 1978; Vol. 5, Chapter 7.
(32) Baraldi, I.; Carnevali, A.; Ponterini, G.; Vanossi, D. *J. Mol. Struct. (THEOCHEM)* **1995**, *333*, 121.
(33) Grant, I. S.; Phillips, W. R. *Electromagnetism*; John Wiley & Sons: Chichester, 1990.
(34) Bartko, A. P.; Dickson, R. M. *J. Phys. Chem. B* **1999**, *103*, 3053.
(35) Sick, B.; Hecht, B.; Novotny, L. *Phys. Rev. Lett.* **2000**, *85*, 4482.

NL049363D